ligand, LPS (23, 24), we observed that the TNF-α and IL-1β expression from monocytes derived from patients with type 2 diabetes diminished after exposure to PGN, Poly I:C, and LPS—ligands of the TLR2, TLR3, and TLR4 receptors, respectively. These data suggest that diabetes perturbs signaling downstream of the TLRs. In this study, we collected $CD14^+$ monocytes from PBMCs via enrichment using magnetic beads; this protocol was used to remove T cells, NK cells, B cells, dendritic cells, and basophils from the PBMC mixture. This is in contrast to the methodology used to isolate these cells in many other studies, in which monocytes were obtained as adherent cells in the culture dish or by a rosetting technique (25, 26). $CD14^+$ cells have been shown to be composed of multiple subtypes of activated states; the classical monocyte-isolation methods used in the other studies might unknowingly remove the fraction of monocytes that are susceptible to apoptosis (27). Over half of the $CD14^+$ diabetic monocytes isolated in this study were dead for 12 h culture even in media containing physiological concentration of glucose (data not shown). Our current data showing attenuation of TLR responsiveness to ligands in diabetic monocytes suggests that initial immune responses that are normally triggered by viruses, bacteria, and parasites could be impaired in diabetes, which is consistent with epidemiological data showing a high incidence of infection in patients with diabetes (3–5).

Gene expression and electron microscopic analysis of monocytes derived from patients with diabetes showed active signatures of ER stress; this is important because ER is an organelle essential for the proper folding and glycosylation of proteins after protein synthesis (28). When cells are under ER stress, protein kinase R-like ER kinase, inositol requiring enzyme 1, and activating transcription factor 6 are activated and function in the adaptation to stress, proper folding of proteins, and removal of harmful unfolded proteins, respectively (29, 30). However, prolonged ER stress leads to apoptotic cell death, which is mediated by CHOP (31). CHOP is a crucial and specific molecule for ER stress-induced apoptosis and alters the transcription of the BCL-2 gene family members (32). The current study showed that diabetic monocytes had increased levels of ER stress-related apoptotic molecules. Moreover, non-diabetic monocytes treated with tunicamycin, an ER stress inducer, underwent apoptosis in a manner similar to monocytes derived from patients with diabetes. From these data, we conclude that ER stress contributes to the susceptibility of diabetic monocytes to apoptosis.

We also observed that tunicamycin-induced ER stress diminished TLR2 and TLR4 signaling without altering expression of TLRs. Tunicamycin induces ER stress by disturbing N-linked glycosylation (33), and previous reports suggest that perturbations in this glycosylation attenuates TLR2 and TLR4 signaling *in vitro* (34, 35). Hence, these data collectively indicate that ER stress may underlie decreases in TLR2 and TLR4 signaling and affect immune function in patients with diabetes.

TLR3 signaling is different from the other TLR signaling pathway; for example, it is independent of MyD88. TLR2 and TLR4 are expressed on the cell surface, whereas TLR3 is expressed in intracellular compartments such as endosomes (13), and its ligands require internalization before signaling occurs. This suggests that disturbances in TLR3 signaling in diabetic monocytes may be due to reasons other than ER stress. Further investigations are needed to elucidate the detailed mechanisms of attenuated TLR signaling in monocytes from patients with diabetes.

ER stress has been shown to be a mainstay of the diabetic condition. Its pathological importance in diabetes is

especially important in pancreatic β-cells, in which glucose toxicity results in ER stress and insufficient insulin secretion (36–38). The current study suggests that monocytes are yet another population of cells vulnerable to hyperglycemia-induced ER stress and dysfunction. Nevertheless, the mechanisms that render pancreatic β-cells and monocytes vulnerable to ER stress in patients with diabetes remain uncertain.

Diabetes is considered a chronic inflammatory disease. Activated macrophages that produce pro-inflammatory cytokines such as TNF-α, IL-1β and IL-6 are thought to contribute to insulin resistance in muscle and adipose tissues (39, 40). Furthermore, the atherosclerotic complications in patients with diabetes have a basis in inflammation; local inflammatory foci in atherosclerotic lesions are commonly composed of foam cells derived from activated macrophages (41, 42). Further studies are needed to determine whether different subpopulations of monocyte-derived cells, for example, systemically circulating and locally residing inflammatory cells, are susceptible to hyperglycemia-induced ER stress and dysfunction.

In conclusion, our findings show that $CD14^+$ monocytes are susceptible to ER stress-induced alterations in inflammatory signaling and apoptosis, which may play a role in the decreased immune function observed in patients with diabetes. Further investigations are needed to discern the mechanisms of diabetes-induced ER stress and perturbations in inflammatory signaling in $CD14^+$ monocytes.

ACKNOWLEDGMENTS

We would like to thank Dr. Iseki for valuable advice and critical comments on electron microscopic examination about ER of monocytes.

REFERENCES

1. Stumvoll M, Goldstein BJ, van Haeften TW. Type 2 diabetes: principles of pathogenesis and therapy. Lancet 2005;365:1333-1346
2. Zimmet P, Alberti KG, Shaw J. Global and societal implications of the diabetes epidemic. Nature 2001;414:782-787
3. Joshi N, Caputo GM, Weitekamp MR, Karchmer AW. Infections in patients with diabetes mellitus. N Engl J Med 1999;341:1906-1912
4. Shah BR, Hux JE. Quantifying the risk of infectious diseases for people with diabetes. Diabetes Care 2003;26:510-513
5. Finney SJ, Zekveld C, Elia A, Evans TW. Glucose control and mortality in critically ill patients. JAMA 2003;290:2041-2047
6. Dunn, GP, Old LJ, Schreiber RD. The immunobiology of cancer immunosurveillance and immunoediting. Immunity 2004;21:137-148
7. Karin M, Lawrence T, Nizet V. Innate immunity gone awry: linking microbial infections to chronic inflammation and cancer. Cell 2006;124:823-835
8. Delamaire M, Maugendre D, Moreno M, Le Goff MC. Impaired leucocyte functions in diabetic patients. Diabet Med 1997;14:29-34
9. Geerlings SE, Hoepelman AI. Immune dysfunction in patients with diabetes mellitus (DM). *FE*MS Immunol Med Microbiol 1999;26:259-265
10. Katz S, Klein B, Elian I, Fishman P, Djaldetti M. Phagocytotic activity of monocytes from diabetic patients. Diabetes Care 1983;6:479-482
11. Geisler C, Almdal T, Bennedsen J, Rhodes JM, Kølendorf K. Monocyte functions in diabetes mellitus. Acta Pathol Microbiol Immunol Scand 1982;[C]90:33-37
12. Takamura T, Honda M, Sakai Y, Ando H, Shimizu A, Ota T, Sakurai M, Misu H, Kurita S, Matsuzawa-Nagata N, Uchikata M, Nakamura S, Matoba R, Tanino M, Matsubara K, Kaneko S. Gene expression profiles in peripheral blood mononuclear cells reflect the pathophysiology of type 2 diabetes. Biochem Biophys Res Commun 2007;361:379-384
13. Akira S, Uematsu S, Takeuchi O. Pathogen recognition and innate immunity. Cell 2006;124:783-801
14. Pasare C, Medzhitov R. Toll-like receptors: linking innate and adaptive immunity. Microbes Infect2004; 6:1382-1387
15. Tateno M, Honda M, Kawamura T, Honda M, Kaneko S. Expression profiling of peripheral-blood mononuclear cells from patients with chronic hepatitis C undergoing interferon therapy. J Infect Dis 2007;195:255-267
16. Stuart LM, Ezekowitz RA. Phagocytosis and comparative innate immunity: learning on the fly. Nat Rev Immunol 2008;8:131-141
17. Thoma-Uszynski S, Stenger S, Takeuchi O, Ochoa MT, Engele M, Sieling PA, Barnes PF, Rollinghoff M, Bolcskei PL, Wagner M, Akira S, Norgard MV, Belisle JT, Godowski PJ, Bloom BR, Modlin RL. Induction of direct antimicrobial activity through mammalian toll-like receptors. Science 2001;291:1544-1547
18. Barton GM, Medzhitov R. Toll-like receptor signaling pathways. Science 2003;300:1524-1525
19. Sabroe I, Parker LC, Dower SK, Whyte MK. The role of TLR activation in inflammation. J Pathol 2008;214:126-135
20. Iwasaki A, Medzhitov R. Toll-like receptor control of the adaptive immune responses. Nat Immunol 2004;10:987-995

21. Ghanim H, Mohanty P, Deopurkar R, Sia CL, Korzeniewski K, Abuaysheh S, Chaudhuri A, Dandona P. Acute modulation of Toll-like receptors by insulin 2008;31:1827-1831.
22. Dasu MR, Devaraj S, Zhao L, Hwang DH, and Jialal I. High glucose induces toll-like receptor expression in human monocytes: mechanism of activation. Diabetes 2008;57:3090-3098
23. Desfaits AC, Serri O, Renier G. Normalization of plasma lipid peroxides, monocyte adhesion, and tumor necrosis factor-alpha production in NIDDM patients after gliclazide treatment. Dibetes care 1998;21:487-493
24. Ohno Y, Aoki N, Nishimura A. In vitro production of interleukin-1, interleukin-6, and tumor necrosis factor-alpha in insulin-dependent diabetes mellitus. J Clin Endocrinol Metab 1993;77:1072-1077
25. Renier G, Mamputu JC, Serri O. Benefits of gliclazide in the atherosclerotic process: decrease in monocyte adhesion to endothelial cells. Metabolism 2003;52:13-18
26. Serbina NV, Jia T, Hohl TM, Pamer EG Monocyte-mediated defense against microbial pathogens. Anne Rev Immunol 2008;26:421-452
27. Wahl LM, Wahl SM, Smythies LE, Smith PD. Isolation of human monocyte populations. Curr Protoc Immunol 2009;7:Unit 7. 6A
28. Ron D, Walter P. Signal integration in the endoplasmic reticulum unfolded protein response. Nat Rev Mol Cell Biol 2007;8:519-529
29. Xu C, Bailly-Maitre B, Reed JC. Endoplasmic reticulum stress: cell life and death decisions. J Clin Invest 2005;115:2656-2664
30. Bukau B, Weisseman J, Horwich A. Molecular chaperones and protein quality control. Cell 2006;125:443-451
31. Wang XZ, Ron D. Stress-induced phosphorylation and activation of the transcription factor CHOP (GADD153) by p38 MAP kinase. Science 1996;272:1347-1349
32. McCullough KD, Martindale JL, Klotz LO, Aw TY, and Holbrook NJ. Gadd153 sensitizes cells to endplasmic reticulum stress by down-regulating Bcl2 and perturbing the cellular redox state. Mol Cell Biol 2001;21:1249-1259
33. Kataoka H, Yasuda M, Iyori M, Kiura K, Narita M, Nakata T, Shibata K. Roles of N-linked glycans in the recognition of microbial lipopeptides and lipoproteins by TLR2. Cell Microbiol 2006;8:1199-1209
34. Ohnishi T, Muroi M, Tanamoto K. N-linked glycosylations at Asn(26) and Asn(114) of human MD-2 are required for toll-like receptor 4-mediated activation of NF-kappaB by lipopolysaccaharide. J Immunol 2001;167:3354-3359
35. Weber AN, Morse MA, Gay NJ. Four N-linked glycosylation sites in human toll-like receptor 2 cooperate to direct efficient biosynthesis and secretion. J Biol Chem 2004;279:34589-34594
36. Ozcan U, Cao Q, Yilmaz E, Lee AH, Iwakoshi NN, Ozdelen E, Tuncman G, Görgün C, Glimcher LH, Hotamisligil GS. Endoplasmic reticulum stress links obesity, insulin action, and type 2 diabetes. Science 2004;306:457-461
37. Oyadomari S, Takeda K, Takiguchi M, Gotoh T, Matsumoto M, Wada I, Akira S, Araki E, Mori M. Nitric oxide-induced apoptosis in pancreatic beta cells is mediated by the endoplasmic reticulum stress pathway. Proc Natl Acad Sci U S A 2001;98:10845-10850
38. Simon S, Maziyar S, Jerrold MO. Insulin sensitivity: modulation by nutrients and inflammation. J Clin Invest 2008;118:2992-3002

39. Kahn SE, Hull RL, Utzschneider KM. Mechanisms linking obesity to insulin resistance and type 2 diabetes. Nature 2006;444:840-846
40. Wellen KE, Hotamisligil GS. Inflammation, stress and diabetes. J Clin Invest 2005;115:1111-1119
41. Brownlee M. Biochemistry and molecular cell biology of diabetic complications. Nature 2001;414:813-820
42. Liang CP, Han S, Senokuchi T, Tall AR. The macrophage at the crossroads of insulin resistance and atherosclerosis. Circ Res 2007;100:1546-1555

Table 1 Characteristics of the study subjects

	Diabetic patients (n=33)	Healthy volunteers (n=28)	P value
Age (years)	62.0±8.6	58.2±10.2	N.S
Gender (male/female)	15/18	15/13	N.S
Body mass index	23.5±4.2	23.6±4.8	N.S
White blood cell counts (/ml)	4800±1700	5600±1900	N.S
Lymphocytes (%)	23.5±3.5	22.7±2.5	N.S
Monocytes (%)	5.2±1.6	6.1±2.3	N.S
Hemoglobin (g/dl)	14.1±1.3	13.6±1.6	N.S
Total cholesterol (mg/dl)	182±24	180±35	N.S
Triglyceride (mg/dl)	138±37	163±33	N.S
FPG (mg/dl)	185±38	86±7.4	<0.001
HbA_{1c} (%)	9.2±2.0	5.4±0.7	<0.001
Diabetic complications (+/-) *	19/14	N.A	
Insulin treatment (+/-)	10/23	N.A	

Data are expressed as means±SD.
* Diabetic complications: nephropathy, neuropathy, retinopathy, macroangiopathy

Table 2 Biological processes for up-regulated genes in monocytes of diabetic patients

MAPP Name	Z Score	Permute P
Golgi-apparatus	3.383	0.000
Ribosomal Proteins	3.691	0.002
Unfold protein binding	2.471	0.026
Intracellular protein transport	2.310	0.029
Enzyme liked receptor protein signaling pathway	2.175	0.042
Nuclear Receptor	2.316	0.043
Gametogenesis	-1.998	0.049

FIGURE LEGENDS

FIG. 1

Monocytes contributed to the vulnerability of the PBMCs in patients with diabetes. (*A*)PBMCs were obtained from 33 patients with diabetes and 28 healthy volunteers. Isolated PBMCs were harvested in AIM-V serum-free culture media supplemented with 5 mM glucose for 3 hours and incubated with FITC-labeled anti-CD4, CD14, or CD56 antibodies, together with PE-labeled Annexin-V to assess the frequency of apoptotic cells in each subpopulation of PBMCs. Apoptotic cells were identified by double-staining with PE-labeled Annexin-V and 7-AAD by flow cytometry. The frequencies of apoptotic cells determined as the Annexin-V-positive and 7-AAD-negative population are expressed as mean ± SEM with statistical comparisons for both groups. The non-parametric Mann-Whitney *U* test was used to calculate the *P* value. $*P < 0.05$ $***P < 0.01$ $***P < 0.001$. The PBMCs of patients with diabetes were more susceptible to apoptosis than those of healthy volunteers, and $CD14^+$ monocytes were contributors. (*B*) Among the 33 patients with diabetes, those with poor glycemic control reflected as $HbA_{1c} \geq 9.0$ were more susceptible to apoptosis in $CD14^+$ monocytes. Data are expressed as mean ± SEM with a statistical comparison of both groups. $*P < 0.05$. (*C*) Monocytes were isolated from 15 patients with $HbA_{1c} \geq 9.0$ and 18 patients with $HbA_{1c} < 9.0$. The expression of the BCL-2 gene in their monocytes before and after incubation in AIM-V serum-free media was assessed by RTD-PCR. After 3 h incubation, the expression of BCL-2 was not upregulated in the poor glycemic control group ($HbA_{1c} \geq 9.0$), as compared to the fair control group ($HbA_{1c} < 9.0$). Data are expressed as mean ± SEM with statistical comparisons of both groups. $*P < 0.05$.

FIG. 2

Attenuated phagocytosis activity in diabetic monocytes. Whole PBMCs were incubated with FITC-labeled *E. coli* for 10 minutes followed by PI staining and flow cytometric analysis. (*A*) Gated PI-positive populations were viable leukocyte populations (upper panel). The monocyte population was assessed using granularity (SSC) and size (FSC) (middle panel). For the gated cells indicating viable monocytes, FITC-positive cells were assessed as monocytes containing phagocytosed FITC-labeled *E. coli.* (lower panel). (*B*) The frequency of monocytes containing phagocytosed *E. coli* in patients with diabetes was less than that in healthy volunteers. Data are expressed as means ± SEM. $*P < 0.05$.

FIG. 3

Hyporesponsiveness to TLR ligand stimuli by the monocytes of patients with diabetes. (*A*)-(*D*) Isolated $CD14^+$ monocytes from 33 patients with diabetes and 28 healthy volunteers were cultured in AIM-V serum-free media supplemented with each TLR ligand: PGN, Poly (I:C), and LPS. After 3 h incubation, RNA was isolated from the monocytes and the expression levels of the TNF-α and IL-1β genes were analyzed by RTD-PCR. The basal (pre-stimuli) expression of (*A*) TLR2, TLR3, and TLR4 and (*B*) TNF-α and IL-1β did not differ significantly between the two groups. The TLR ligand-induced expression of (*C*) TNF-α and (*D*) IL-1β was downregulated in the monocytes of patients with diabetes. Data are expressed as means ± SEM. $*P < 0.05$, $**P < 0.01$.

FIG. 4

Monocytes of patients with diabetes were under ER stress. (*A*) The gene expression profiles of representative vulnerable CD14$^+$ monocytes obtained from five patients with diabetes and five healthy volunteers were analyzed using a DNA microarray. Unsupervised hierarchical clustering using 17,184 filtered genes produced two clusters that separated the patients with diabetes from the healthy volunteers without exception. (*B*)–(*C*), The gene expression levels of the ER stress markers, such as CHOP and BiP, on CD14$^+$ monocytes and CD4$^+$ T cells obtained from 33 patients with diabetes and 28 healthy volunteers was analyzed using RTD-PCR. (*B*) The expression levels of CHOP and BiP in monocytes of patients with diabetes were significantly upregulated, as compared to the monocytes of healthy volunteers. Data are expressed as means ± SEM. $*P < 0.05$, $**P < 0.01$. (*C*) The expression levels of CHOP and BiP in T cells of patients with diabetes were similar to those of healthy volunteers. Data are expressed as mean ± SEM. (*D*) Monocytes were obtained from three healthy volunteers and three patients with diabetes (Healthy volunteer 1: 64-year-old man, HbA_{1c} 5.7%; Healthy volunteer 2: 66-year-old man, HbA_{1c} 4.9%; Healthy volunteer 3: 68-year-old woman, HbA_{1c} 5.6%; Diabetic patient 1: 56-year-old man, HbA_{1c} 9.1%; Diabetic patient 2: 64-year-old woman, HbA_{1c} 8.2%; Diabetic patient 3: 71-year-old man, HbA_{1c} 10.2%) and examined them using electron microscopy. In the three patients with diabetes, the concentric, continuous, and regular layer structures of the ER were corrupted, with fewer ribosomes on the ER membrane compared to the ER of the healthy volunteer. ER, endoplasmic reticulum; N, nucleus; M, mitochondrion. Scale bars indicate 100 nm.

FIG. 5

ER stress enhanced the susceptibility of human monocytes to apoptosis. (*A*)–(*B*) Human CD14$^+$ monocytes obtained from a healthy volunteer were incubated in AIM-V culture media supplemented with tunicamycin (1 or 5 μg/ml). The frequency of apoptotic cells was analyzed by flow cytometry every 3 h for 12 h. More apoptotic cells were observed among monocytes treated with tunicamycin for more than 6 h incubation, as compared to untreated monocytes. (*A*) Representative scattergram of Annexin-V and 7-AAD for monocytes treated with tunicamycin. The numbers in each quadrant indicate the percentage of apoptotic cells. (*B*) Apoptotic cells were assessed in triplicate for each condition. Data are expressed as means ± SEM. (*C*) Caspse-3 activity in monocytes treated with tunicamycin increased significantly at 12 h incubation. (*D*) The BCL-2 expression in monocytes incubated with tunicamycin for 12 h was down-regulated. (*E*) The expression levels of the ER stress markers CHOP and BiP in monocytes incubated with tunicamycin for 12 h were significantly up-regulated. Data are expressed as means ± SEM of three independent experiments. Open bars, no treatment; shaded bar, treatment with tunicamycin (1 μg/ml); solid bar, treatment with tunicamycin (5 μg/ml). TM, tunicamycin.

FIG. 6

Expression of pro-inflammatory cytokines in response to TLR ligand stimuli decreased in human monocytes treated with tunicamycin. Isolated human CD14$^+$ monocytes were incubated in AIM-V culture media with tunicamycin (1 or 5 μg/ml) and stimulated using TLR ligands, PGN, and LPS for 6 h. *A–C*, RTD-PCR analysis showed that the expression of TNF-α (*A*), IL-1β (*B*),

and IL-6 (*C*) was down-regulated in human CD14$^+$ monocytes treated with tunicamycin, especially at the higher concentration (5 μg/ml). *D–F*, ELISA showed that the production of TNF-α (*D*), IL-1β (*E*), and IL-6 (*F*) in culture media decreased in human monocytes treated with tunicamycin, especially at the higher concentration (5 μg/ml). Data are expressed as means ± SEM of four independent experiments. Open bars, no treatment; shaded bar, treatment with tunicamycin (1 μg/ml); solid bar, treatment with tunicamycin (5 μg/ml). TM, tunicamycin.

Figure 1

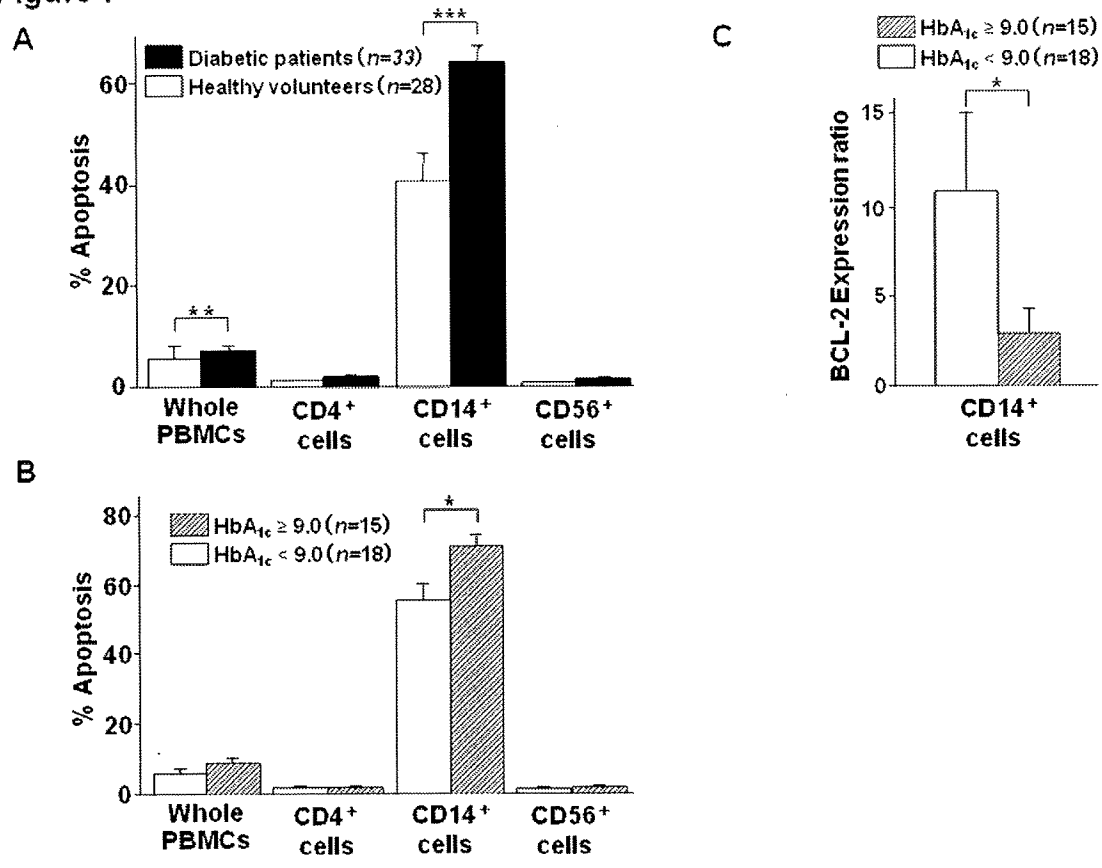

Figure 2

A

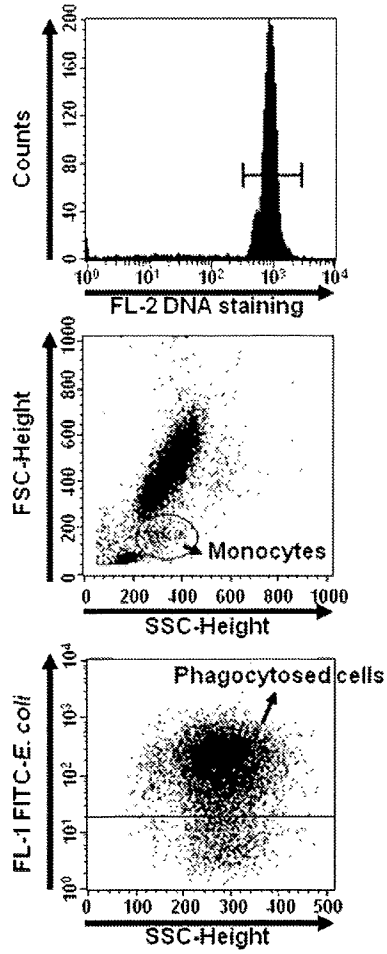
Counts
FL-2 DNA staining
FSC-Height
Monocytes
SSC-Height
FL-1 FITC-E. coli
Phagocytosed cells
SSC-Height

B

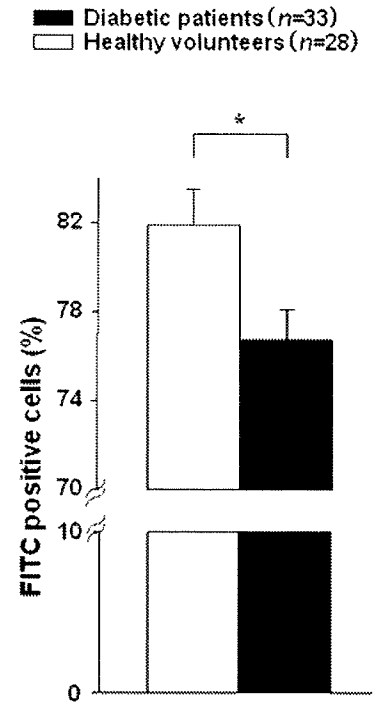
Diabetic patients (n=33)
Healthy volunteers (n=28)
*
FITC positive cells (%)
82
78
74
70
10
0

Figure 3

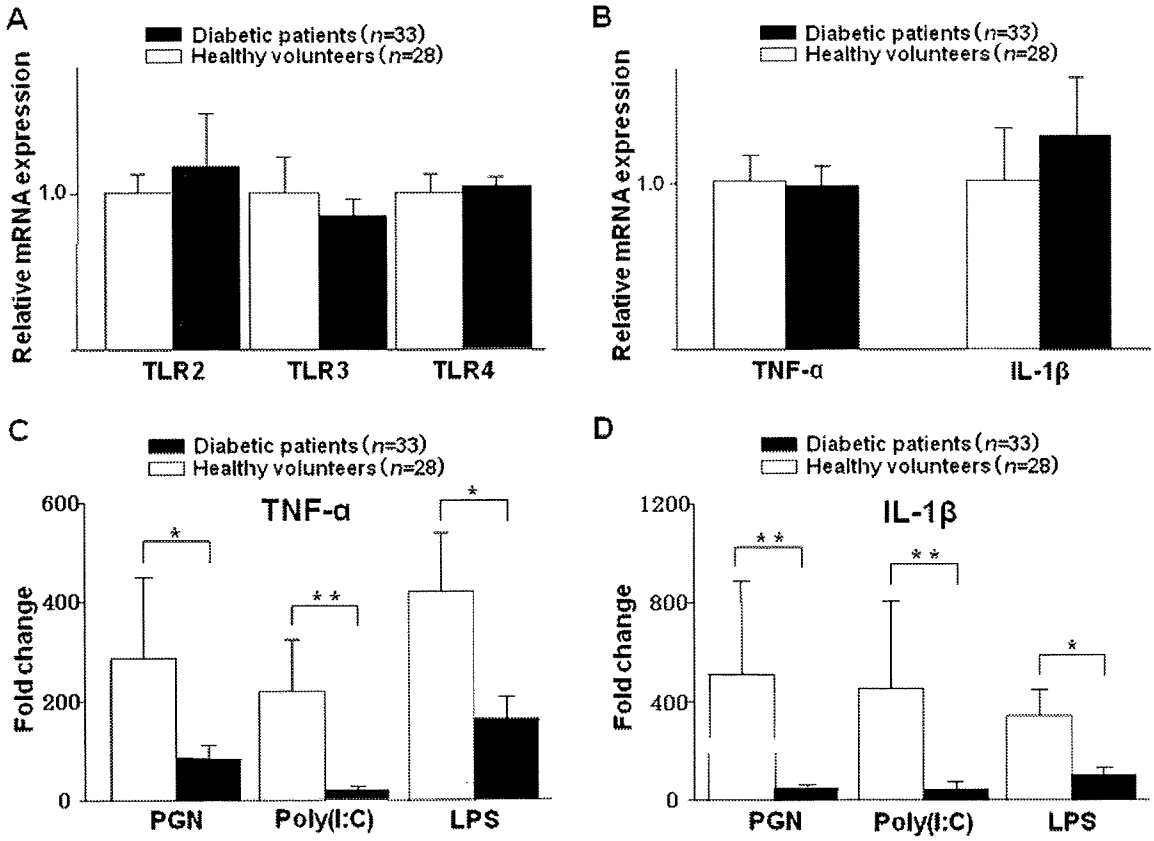
A
Diabetic patients (n=33)
Healthy volunteers (n=28)
Relative mRNA expression
1.0
TLR2
TLR3
TLR4
B
Diabetic patients (n=33)
Healthy volunteers (n=28)
Relative mRNA expression
1.0
TNF-α
IL-1β
C
Diabetic patients (n=33)
Healthy volunteers (n=28)
TNF-α
Fold change
600
400
200
0
*
**
*
PGN
Poly(I:C)
LPS
D
Diabetic patients (n=33)
Healthy volunteers (n=28)
IL-1β
Fold change
1200
800
400
0
**
**
*
PGN
Poly(I:C)
LPS

Figure 4

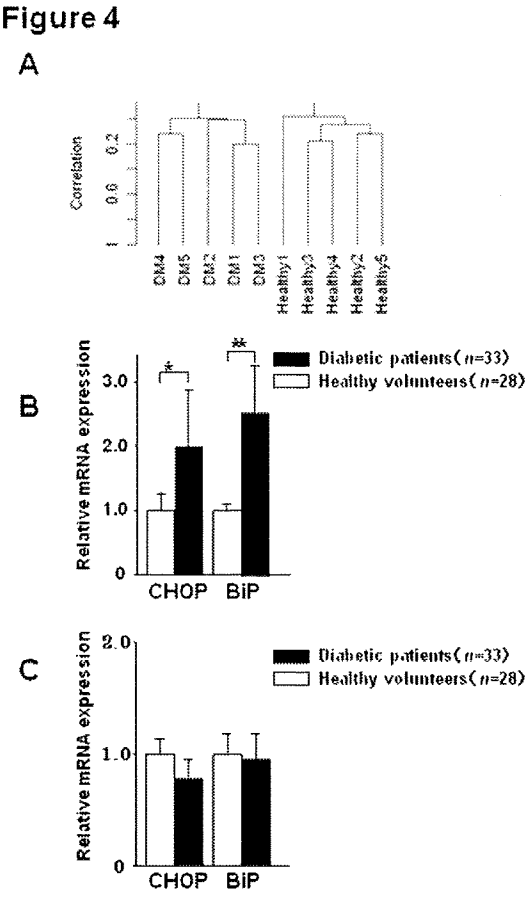
A
Correlation
1
0.6
0.2
DM4
DM5
DM2
DM1
DM3
Healthy1
Healthy3
Healthy4
Healthy2
Healthy5
B
Relative mRNA expression
3.0
2.0
1.0
0
*
**
Diabetic patients(n=33)
Healthy volunteers(n=28)
CHOP
BiP
C
Relative mRNA expression
2.0
1.0
0
Diabetic patients(n=33)
Healthy volunteers(n=28)
CHOP
BiP

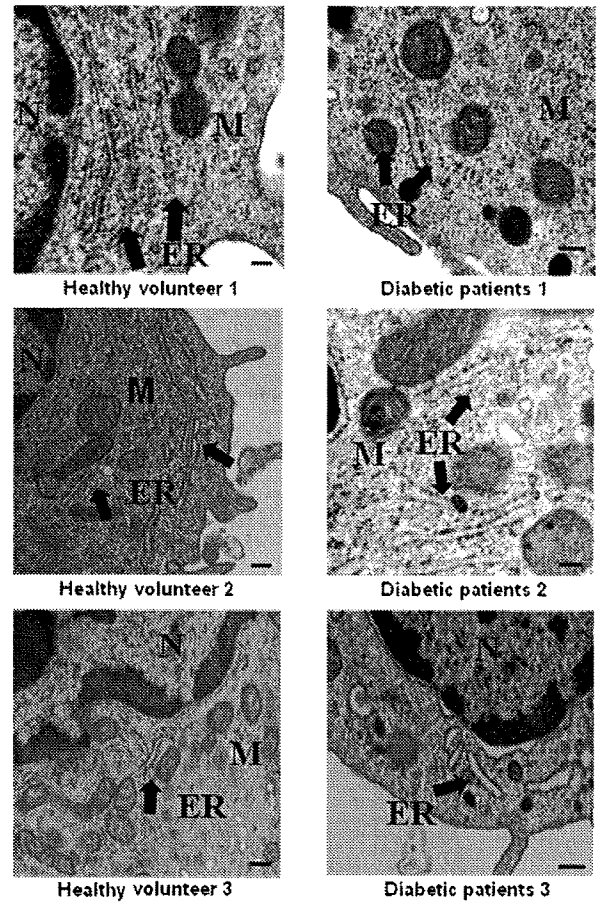
D
N
M
ER
Healthy volunteer 1
Diabetic patients 1
Healthy volunteer 2
Diabetic patients 2
Healthy volunteer 3
Diabetic patients 3

Figure 5

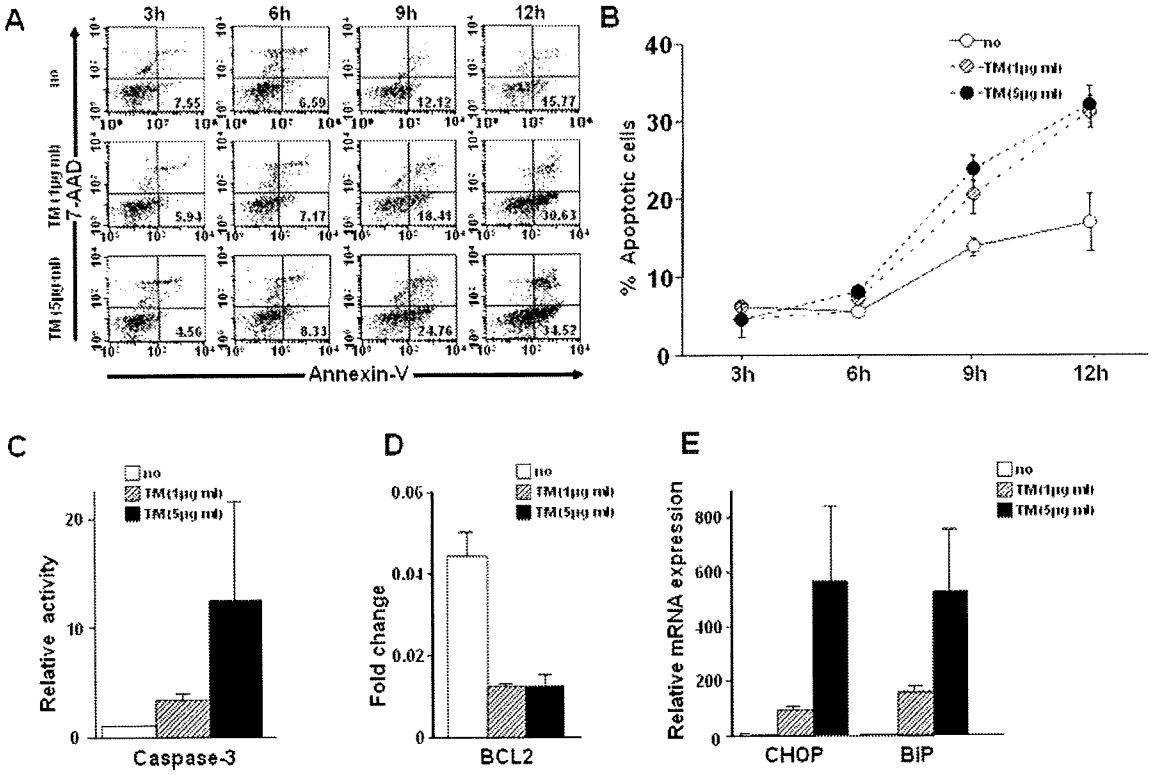
A
3h
6h
9h
12h
no
TM (1μg ml)
TM (5μg ml)
7-AAD
Annexin-V
7.55
6.59
12.12
15.77
5.93
7.17
18.41
30.63
4.56
8.33
24.76
34.52
B
% Apoptotic cells
no
TM(1μg ml)
TM(5μg ml)
C
Relative activity
Caspase-3
D
Fold change
BCL2
E
Relative mRNA expression
CHOP
BiP

Figure 6

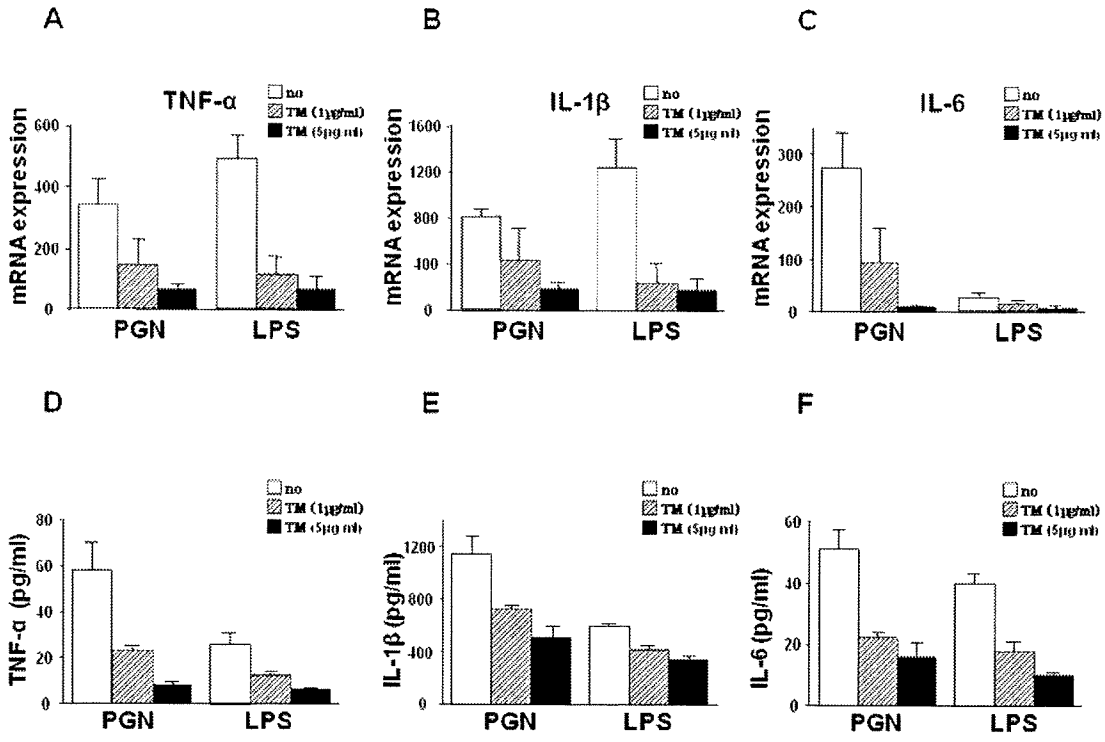
A
TNF-α
mRNA expression
PGN
LPS
B
IL-1β
mRNA expression
PGN
LPS
C
IL-6
mRNA expression
PGN
LPS
D
TNF-α (pg/ml)
PGN
LPS
E
IL-1β (pg/ml)
PGN
LPS
F
IL-6 (pg/ml)
PGN
LPS

Differential MicroRNA Expression Between Hepatitis B and Hepatitis C Leading Disease Progression to Hepatocellular Carcinoma

Shunsuke Ura,[1] Masao Honda,[1,2] Taro Yamashita,[1] Teruyuki Ueda,[1] Hajime Takatori,[1] Ryuhei Nishino,[1] Hajime Sunakozaka,[1] Yoshio Sakai,[1] Katsuhisa Horimoto,[3] and Shuichi Kaneko[1]

MicroRNA (miRNA) plays an important role in the pathology of various diseases, including infection and cancer. Using real-time polymerase chain reaction, we measured the expression of 188 miRNAs in liver tissues obtained from 12 patients with hepatitis B virus (HBV)-related hepatocellular carcinoma (HCC) and 14 patients with hepatitis C virus (HCV)-related HCC, including background liver tissues and normal liver tissues obtained from nine patients. Global gene expression in the same tissues was analyzed via complementary DNA microarray to examine whether the differentially expressed miRNAs could regulate their target genes. Detailed analysis of the differentially expressed miRNA revealed two types of miRNA, one associated with HBV and HCV infections (n = 19), the other with the stage of liver disease (n = 31). Pathway analysis of targeted genes using infection-associated miRNAs revealed that the pathways related to cell death, DNA damage, recombination, and signal transduction were activated in HBV-infected liver, and those related to immune response, antigen presentation, cell cycle, proteasome, and lipid metabolism were activated in HCV-infected liver. The differences in the expression of infection-associated miRNAs in the liver correlated significantly with those observed in Huh7.5 cells in which infectious HBV or HCV clones replicated. Out of the 31 miRNAs associated with disease state, 17 were down-regulated in HCC, which up-regulated cancer-associated pathways such as cell cycle, adhesion, proteolysis, transcription, and translation; 6 miRNAs were up-regulated in HCC, which down-regulated anti-tumor immune response. *Conclusion:* miRNAs are important mediators of HBV and HCV infection as well as liver disease progression, and therefore could be potential therapeutic target molecules. (HEPATOLOGY 2009;49:1098-1112.)

MicroRNA (miRNA) is an endogenous, small, single-strand, noncording RNA consisting of 20 to 25 bases and regulates gene expression of various cell types. It plays an important role in various biological processes, including organ development and differentiation as well as cellular death and proliferation, and is also involved in various diseases such as infection and cancer.[1-3]

miRNAs are produced as follows. A primary miRNA with a hairpin loop structure is cleaved into a precursor miRNA and transported out of the nuclei with a carrier protein (Exportin-5). The precursor miRNA is then processed by Dicer and converted into an active single-strand RNA in the cytoplasm. The miRNA binds to a target messenger RNA in a sequence-dependent manner and induces degradation of the target messenger RNA and translational inhibition. One miRNA regulates the expression of multiple target genes; bioinformatics analyses have suggested that the expression of more than 30% of human genes is regulated by miRNAs.[4-7]

Abbreviations: cDNA, complementary DNA; CH, chronic hepatitis; CH-B, chronic hepatitis B; CH-C, chronic hepatitis C; HBV, hepatitis B virus; HCC, hepatocellular carcinoma; HCC-B, hepatitis B-related hepatocellular carcinoma; HCC-C, hepatitis C-related hepatocellular carcinoma; HCV, hepatitis C virus; miRNA, microRNA; RTD-PCR, real-time detection polymerase chain reaction; SVM, support vector machine.

From the Departments of [1]Gastroenterology and [2]Advanced Medical Technology, Kanazawa University Graduate School of Medicine, Kanazawa, Japan; and the [3]Biological Network Team, Computational Biology Research Center, National Institute of Advanced Industrial Science and Technology, 2-42 Aomi, koto-ku, Tokyo 135-0064, Japan.

Received July 3, 2008; accepted November 15, 2008.

Address reprint requests to: Masao Honda, M.D., Ph.D., Department of Gastroenterology, Graduate School of Medicine, Kanazawa University, Takara-Machi 13-1, Kanazawa 920-8641, Japan. E-mail: mhonda@m-kanazawa.jp; fax: (81)-76-234-4250.

Published online in Wiley InterScience (www.interscience.wiley.com).

DOI 10.1002/hep.22749

Potential conflict of interest: Nothing to report.

Additional Supporting Information may be found in the online version of this article.

Table 1. Characteristics of Patients Used for Analysis of miRNA and Microarray Samples

Patient No.	Virus	Age	Sex	ALT	Histology of Activity	Background Liver Fibrosis	Histological Grade of HCC	Tumor Size (mm)	TNM Staging	HCV-RNA (KIU/mL)	HBV-DNA (LEG/mL)
1	HBV	57	M	16	2	4	Moderate	20	II	–	3.4
2	HBV	51	M	57	1	2	Moderate	48	II	–	< 2.6
3	HBV	61	M	17	1	4	Well	16	II	–	< 3.7
4	HBV	47	M	19	1	4	Moderate	15	I	–	< 3.7
5	HBV	72	M	19	1	1	Well	25	II	–	NA
6	HBV	73	M	62	1	3	Moderate	45	III	–	5.7
7	HBV	42	M	36	1	4	Moderate	18	I	–	< 3.7
8	HBV	63	M	13	1	2	Moderate	15	I	–	2.8
9	HBV	68	F	54	1	2	Well	56	II	–	4.1
10	HBV	70	M	13	0	2	Well	40	II	–	< 3.7
11	HBV	58	M	29	1	4	Moderate	35	IVA*	–	3.3
12	HBV	72	M	22	1	4	Moderate	18	I	–	6
13	HCV	66	F	33	2	4	Well	25	II	423	–
14	HCV	67	M	89	1	4	Well	30	II	> 850	–
15	HCV	64	M	31	1	4	Moderate	75	III	< 5 (+)	–
16	HCV	68	M	30	0	4	Well	23	II	> 850	–
17	HCV	46	M	98	2	3	Moderate	20	I	> 850	–
18	HCV	68	F	32	2	4	Moderate	25	III	< 5 (+)	–
19	HCV	66	F	46	2	4	Well	25	II	> 850	–
20	HCV	47	M	246	1	3	Moderate	20	I	262	–
21	HCV	75	M	27	1	3	Moderate	19	II	85.1	–
22	HCV	77	M	21	0	1	Moderate	20	II	< 5 (−)	–
23	HCV	66	M	46	2	2	Well	60	II	50.3	–
24	HCV	65	M	89	1	1	Poorly	25	III	850	–
25	HCV	53	M	54	0	1	Moderate	28	II	< 5 (−)	–
26	HCV	75	F	212	1	4	Well	19	I	580	–
27	–	51	F	18	0	0	–	–	–	–	–
28	–	78	F	13	0	0	–	–	–	–	–
29	–	75	M	20	0	0	–	–	–	–	–
30	–	34	M	12	0	0	–	–	–	–	–
31	–	64	M	30	0	0	–	–	–	–	–
32	–	78	M	9	0	0	–	–	–	–	–
33	–	53	M	19	0	0	–	–	–	–	–
34	–	64	F	12	0	0	–	–	–	–	–
35	–	60	F	20	0	0	–	–	–	–	–

HCV RNA was assayed via Amplicor Monitor Test (KIU/mL); HBV DNA was assayed via transcription-mediated amplification (LEG/mL).

Abbreviations: ALT, alanine aminotransferase; F, female; HBV, hepatitis B virus; HCC, hepatocellular carcinoma; HCV, hepatitis C virus; M, male; TNM, tumor-node–metastasis.

*Vascular invasion (+).

Infection of the human liver with hepatitis B virus (HBV) and hepatitis C virus (HCV) induces the development of chronic hepatitis (CH), cirrhosis, and in some instances hepatocellular carcinoma (HCC).[8] The virological features of these two distinct viruses are completely different; however, the viruses infect the liver and cause CH, which is not distinguished by histological examination or clinical manifestations. We previously reported that gene expression profiles in chronic hepatitis B (CH-B) and chronic hepatitis C (CH-C) are different. Proapoptotic and DNA repair responses were predominant in CH-B, and inflammatory and antiapoptotic phenotypes were predominant in CH-C. However, factors inducing these differences in gene expression remain to be elucidated.[9,10]

We examined miRNA expression in liver tissue with HBV-related liver disease (CH-B and HCC-B) and HCV-related liver disease (CH-C and HCC-C) and in normal liver tissue via real-time detection polymerase chain reaction (RTD-PCR). We also performed global analysis of messenger RNA expression in these tissues using complementary DNA (cDNA) microarray. These analyses allowed us to find characteristic miRNAs associated with HBV or HCV infection as well as the progression of liver disease.

Patients and Methods

Patients. The study subjects included 12 patients with CH-B complicated by HCC and 14 patients with

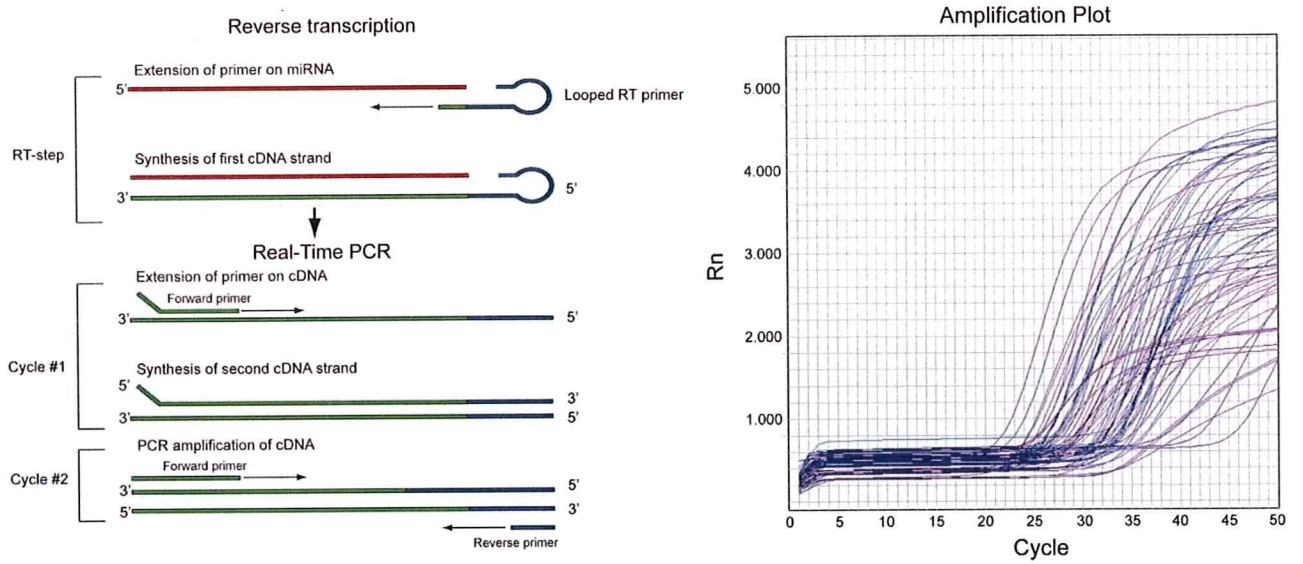

Fig. 1. (A) miRNA-specific RTD-PCR using sheet hairpin primers. (B) miRNA amplification curves by RTD-PCR.

CH-C complicated by HCC. Gene expression analysis was approved by the ethics committee of the Graduate School of Medicine, Kanazawa University Hospital, Japan, between 1999 and 2004. In addition, nine normal liver tissue samples obtained during surgery for metastatic liver cancer were used as control samples. Surgically removed liver tissues were stored in liquid nitrogen until analysis. Histological classification of HCC and histological evaluation of hepatitis in noncancerous regions for each patient are shown in Table 1. HCV viremia in two patients with CH-C was persistently cleared by interferon therapy before HCC development. There were no significant differences in the histological findings of HCC and noncancerous regions, as well as in sex, age, and hepatic function between the HBV and HCV infection groups.

Quantitative RTD-PCR. Approximately 1 mg of each liver tissue sample stored in liquid nitrogen was ground with a homogenizer while still frozen, and total RNA containing miRNA was isolated according to the protocol of the mirVana miRNA Isolation kit (Ambion, Austin, TX) and stored at −80°C until analysis. miRNA expression levels were quantitated using the TaqMan MicroRNA Assays Human Panel Early Access kit (Applied Biosystems, Foster City, CA). cDNA was prepared via reverse transcription using 10 ng each of the isolated total RNA and 3 μL each of the reverse transcription primers with specific loop structures. Reverse transcription was performed using the TaqMan MicroRNA Reverse Transcription kit (Applied Biosystems) according to the manufacturer's protocol. Then, a mixture of 6.67 μL of nuclease-free water, 10 μL of TaqMan 2 × Universal PCR Master Mix (No AmpErase UNG; Applied Biosystems), and 2 μL of TaqMan MicroRNA Assay Mix, which was included in the kit, was prepared for each sample on a 384-well plate; 1.33 μL of the reverse transcription product was added to the mixture, and amplification reaction was performed on an ABI PRISM 7900HT (Applied Biosystems). Expression levels of 188 miRNAs in each sample were quantitated.

Analysis of RTD-PCR Data. The measured 188 miRNAs included RNU6B, which is commonly used as a control for miRNA. β-Actin and glyceraldehyde 3-phosphate dehydrogenase were also measured simultaneously for correcting RNA amount. The mean Ct values and standard deviations of each miRNA were calculated from expression data of all patients obtained by RTD-PCR. miRNA with the lowest expression variation was used as the internal control. Ct values of each miRNA were then corrected by the Ct value of the internal control to yield −ΔCt values defined as relative miRNA expression levels and used for analyses. Statistical analyses and hierarchical cluster analyses of expression data were performed using BRB ArrayTools (http://linus.nci.nih.gov/BRB-ArrayTools.html). Relative miRNA expression levels were further normalized using the median over the all patients so that the normalized expression levels of each patient have a median log ratio of 0. A class prediction method was used for classifying two patient groups based on the supervised learning method, and a binary tree classification method was used for classifying three or more patient groups with a statistical algorithm of the support vector machine (SVM). Class prediction was performed using SVM incorporating genes differentially expressed at a univariate parametric significance level of $P = 0.01$. The prediction rate was estimated via cross-validation and the bootstrap method for small sample data.[11] (It is worth

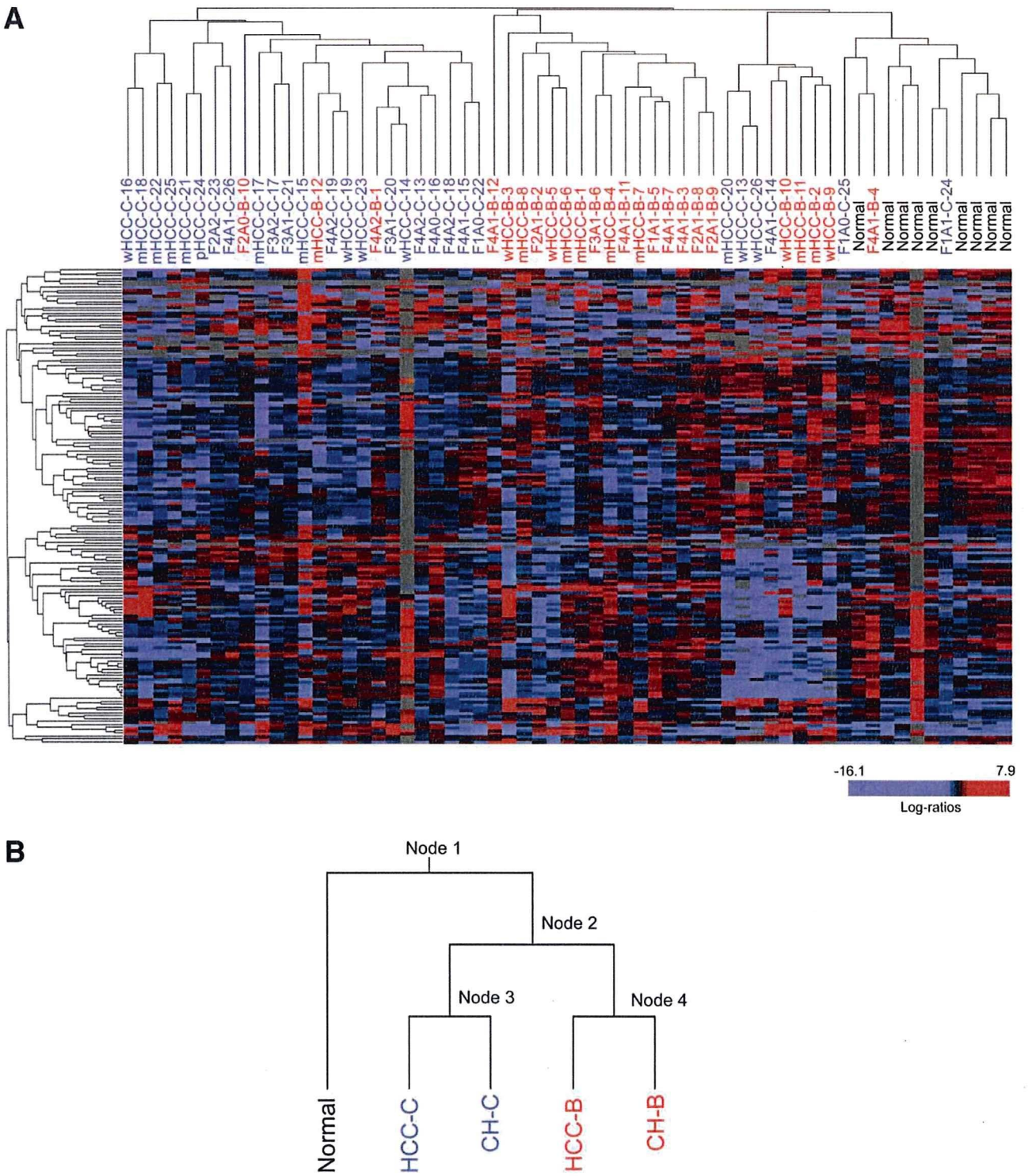

Fig. 2. (A) Hierarchical cluster analysis using total miRNA. Chronic hepatitis is indicated by histological stage and grade (F, fibrosis; A, activity) and type of infecting virus (B or C). HCC is indicated by histological grade (w, well differentiated; m, moderately differentiated; p, poorly differentiated) and type of infecting virus (B or C), with the patient number added at the end. (B) Relationship between five classes divided by binary tree classification. Expression profiles were first classified into normal liver and non-normal liver groups (node 1), then into HBV and HCV groups (node 2). The HBV group was further divided into HCC-B and CH-B (node 3), and the HCV group into HCC-C and CH-C (node 4).

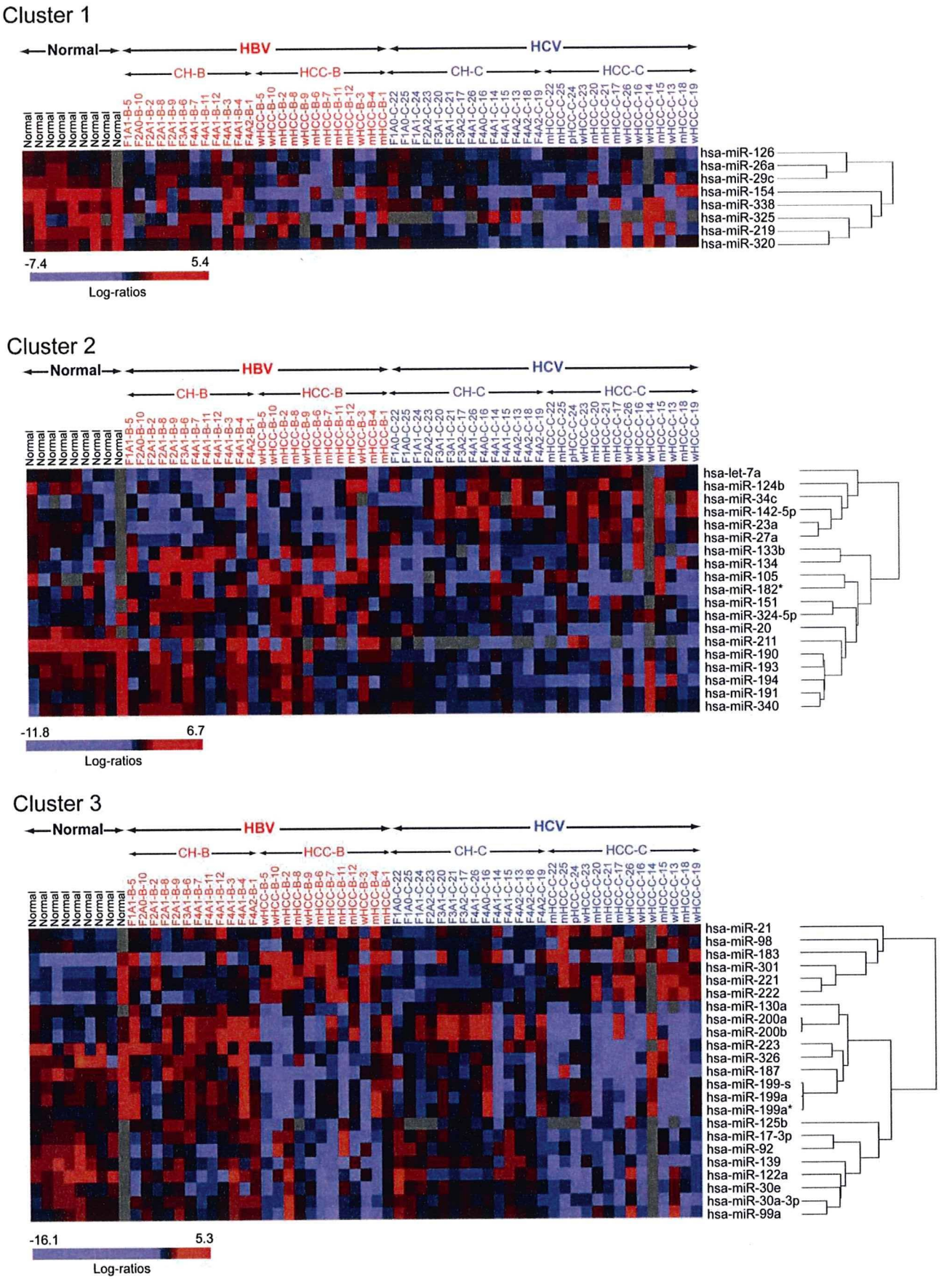

Fig. 3. Cluster 1: Eight miRNAs specifically differentiated node 1 classification. Cluster 2: Nineteen miRNAs specifically differentiated node 2 classification. Cluster 3: Twenty-three miRNAs differentiated CH-B and HCC-B as well as CH-C and HCC-C.

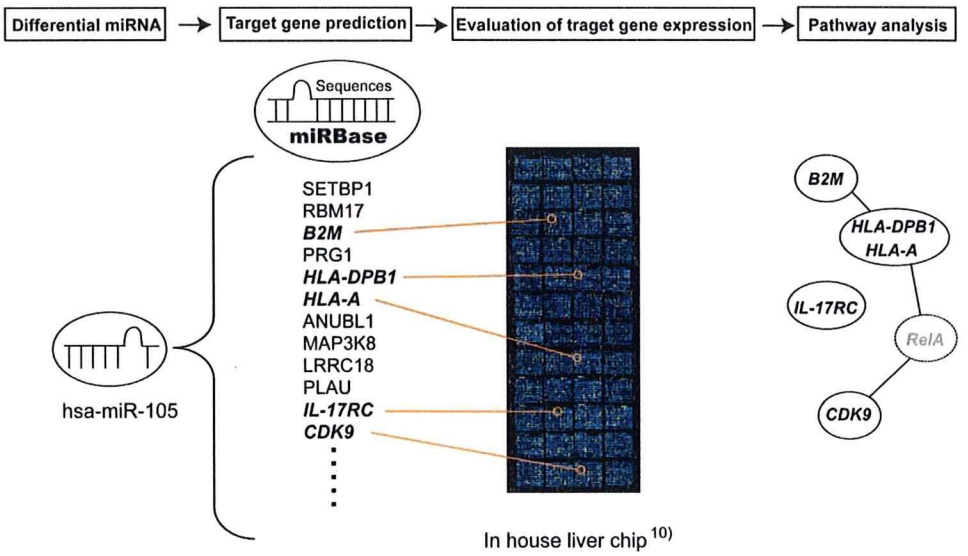

Fig. 4. Analysis of miRNA expression data. Target genes of miRNAs were predicted using MIRANDA Pro3.0; candidate target genes spotted on microarray were identified; number of genes that actually exhibit significant ($P < 0.05$) changes in expression among the genes was determined; and signal pathways involving genes regulated by the miRNAs that had exhibited differential expression between each group were analyzed using MetaCore (Table 4).

noting that the prediction rate may be likely an overestimate of the true rate, given the weaknesses of cross-validation and bootstrapping methods in a strict sense.)

Microarray Analysis. cDNA microarray slides (Liver chip 10k) were used as described.[10] RNA isolation, amplification of antisense RNA, labeling, and hybridization were performed according to the protocols described.[9,10] Quantitative assessment of the signals on the slides was performed by scanning on the ScanArray 5000 (General Scanning, Watertown, MA) followed by image analysis using GenePix Pro 4.1 (Axon Instruments, Union City, CA) as described.[10]

Preliminary Survey of Independency of Paired Samples from the Same Patient. CH and HCC expression data were derived from the same patient. Before further analysis, we examined whether the miRNA expression of paired samples was similar or independent. We compared differences in the expressions of paired and nonpaired CH and HCC samples using the Dunnett test[12] (Supplementary Data). All possible tests performed for data pairs represented no dependency due to the paired data from the same patients. For data analysis, we used the standard pairwise class comparison and prediction tool in BRB ArrayTools.

Identification of Candidate miRNA Target Genes. Candidate target genes predicted to be regulated by miRNAs based on sequence comparison were selected using MIRANDA Pro3.0 (Sanger Institute). Of the selected genes, those represented on a microarray chip were then examined for expression (Fig. 4). The number of genes showing a significant ($P < 0.05$) expression difference among the candidate target genes represented on the chip was statistically analyzed to evaluate the significance of expression regulation by miRNAs. Analysis of significance was performed using Hotelling T2 test (BRB ArrayTools).

Pathway Analysis. Of the candidate miRNA target genes, those showing a significant ($P < 0.01$) expression difference between N, CH-B, HCC-B, CH-C, and HCC-C samples were analyzed for pathways involving these genes using MetaCore software suite (GeneGo, St. Joseph, MI). Significance probability was calculated using

Table 2-1. Class Prediction

No.	Class	Prediction (%)	No. of Predictors	*P* Value
1	HBV versus HCV	87	32	<0.001
2	N versus CH (B+C)	91	26	0.007
3	CH (B+C) versus HCC (B+C)	92	34	0.003

Class prediction algorithm was used for the classification of two groups of patients. Feature selection was based on the univariate significance level (alpha = 0.01). The support vector machine classifier was used for class prediction.

Abbreviations: CH, nontumor lesion of HCC; HCC, hepatocellular carcinoma; N, normal.

Table 2-2 Binary Tree Classification

Node	Group 1 Class	Group 2 Class	No. of Predictors	Misclassification Rate (%)
1	HCC-B, HCC-C, CH-B, CH-C	N	20	4.9
2	HCC-B, CH-B	HCC-C, CH-C	19	13.5
3	HCC-B	CH-B	15	29.2
4	HCC-C	CH-C	14	17.9

Binary tree classification algorithm was used for the classification of each category of patients. Feature selection was based on the univariate significance level (alpha = 0.01). The support vector machine classifier was used for class prediction. There were four nodes in the classfication tree.

Abbreviations: CH-B, non-tumor lesion of HCC-B; CH-C, nontumor lesion of HCC-C; HCC-B, hepatitis B virus-related hepatocellular carcinoma; HCC-C, hepatitis C virus-related hepatocellular carcinoma; N, normal